

論文 / 著書情報  
Article / Book Information

Title(English)	A fault-zone conductor beneath a compressional inversion zone, northeastern Honshu, Japan
Authors(English)	Ichihara, H., M. Uyeshima, S. Sakanaka, T. Ogawa, M. Mishina, Y. Ogawa, T. Nishitani, Y. Yamaya, A. Watanabe, Y. Morita, R. Yoshimura, Y. Usui
Citation(English)	Geophys. Res. Lett., 38, , L09301
Pub. date	2011, 5

## A fault-zone conductor beneath a compressional inversion zone, northeastern Honshu, Japan

Hiroshi Ichihara,<sup>1,2</sup> Makoto Uyeshima,<sup>1</sup> Shinya Sakanaka,<sup>3</sup> Tsutomu Ogawa,<sup>1</sup> Masaaki Mishina,<sup>4</sup> Yasuo Ogawa,<sup>5</sup> Tadashi Nishitani,<sup>3</sup> Yusuke Yamaya,<sup>1,6</sup> Atsushi Watanabe,<sup>1</sup> Yuichi Morita,<sup>1</sup> Ryokei Yoshimura,<sup>7</sup> and Yoshiya Usui<sup>1</sup>

Received 17 March 2011; accepted 28 March 2011; published 3 May 2011.

[1] A resistivity section based on magnetotelluric data was obtained for the Shonai Plain fault in northeastern Honshu, Japan. Faults in this area were created as normal faults during the opening of the Japan Sea in the Miocene but are now reactivated as high-angle reverse faults under compressional tectonics. Geological interpretations of the resistivity section support the proposed fault reactivation. An estimated east-dipping conductor along a deep part of the Shonai Plain fault system probably represents a fluid-rich zone around the fault zone. The high <sup>3</sup>He/<sup>4</sup>He ratio near the fault indicates transportation of mantle fluid through this fluid-rich zone. These evidences may reflect the development of pronounced fracture permeability after fault rupturing, as in the fault-valve hypothesis. **Citation:** Ichihara, H., et al. (2011), A fault-zone conductor beneath a compressional inversion zone, northeastern Honshu, Japan, *Geophys. Res. Lett.*, 38, L09301, doi:10.1029/2011GL047382.

### 1. Introduction

[2] Imaging of fluid distribution in seismogenic faults is essential to understanding fault-rupture processes because pore fluids control the shear fracture strength and the brittle-ductile behavior of rocks. Northeastern Honshu is one of the best areas to examine the relationship between fault rupture and fluid behavior. In this area, as shown in Figure 1a, compressional tectonic inversion has caused numerous damaging inland earthquakes, such as the 2004 Chuetsu earthquake (*M* 6.8), the 2007 Chuetsu-oki earthquake (*M* 6.8), and the 2008 Iwate-Miyagi earthquake (*M* 7.2). The earthquake-producing faults originally formed as normal faults during back-arc opening of the Japan Sea (15–25 Ma). Since then, a compressional tectonic regime has developed (3.5 Ma), and the faults are now reactivated as reverse faults [e.g., Sato, 1994] in contractional zones. To explain the reactivation, fluid over-pressuring that reduces frictional strength

has been suggested because fault dips, in terms of earthquake mechanisms [e.g., Hikima and Koketsu, 2005], are too high (>45 degrees) to reactivate the faults in many cases [e.g., Sibson, 2007, 2009].

[3] Because electrical resistivity depends strongly on the pore-fluid distribution, salinity, and connectivity of fluid-filled rock pores, fluid distribution in fault zones has been studied using resistivity imaging [e.g., Ichihara et al., 2009; Wannamaker et al., 2009]. Past magnetotelluric (MT) surveys in fault reactivation zones have identified conductors beneath seismogenic zones, which imply local accumulation of stress and the potential to generate intraplate earthquakes [Ogawa et al., 2001; Uyeshima et al., 2005; Yoshimura et al., 2008]. However, fluid distribution in reactivated faults has not been well understood. To elucidate the relationship between fluid and fault rupture, this study used wide-band MT surveys to model electrical resistivity distribution across the Shonai Plain fault system (Figure 1b), a typical compressional inversion zone [Sato, 1994]. The fault system includes Holocene reverse faults and has experienced large, destructive earthquakes, such as the 1894 Shonai earthquake (*M*7.0) [Awata and Kakimi, 1985].

### 2. Magnetotelluric Measurements and Data Processing

[4] Eleven MT stations were established along a 50-km profile across the Shonai Plain fault zone in September and November 2008 (Figure 1b). Time-series MT data were recorded using an MTU2000 system (Phoenix Geophysics Ltd.). Electric fields at all sites were measured using Pb-PbCl<sub>2</sub> electrodes, and magnetic fields were measured using three mutually orthogonal induction coils. The time-series data were converted to a frequency-domain impedance tensor between 320 and 0.00034 Hz. The remote reference technique [Gamble et al., 1979] was applied in the data processing using horizontal magnetic field data from Sawauchi Station, approximately 100 km north of the study area, which yielded a high-quality MT response and geomagnetic tipper (Figure 2 and Figure S1 of the auxiliary material).<sup>1</sup>

### 3. Two-Dimensional Inversion of MT Data

[5] To evaluate the two-dimensional (2-D) strike direction of MT data, MT phase-tensor analysis [Caldwell et al., 2004] was applied. Phase-tensor analysis is an important tool for recognizing the dimensionality of the subsurface structure without the effect of galvanic distortion. The MT

<sup>1</sup>Earthquake Research Institute, University of Tokyo, Tokyo, Japan.

<sup>2</sup>Japan Agency for Marine-Earth Science and Technology, Yokosuka, Japan.

<sup>3</sup>Faculty of Engineering and Resource Science, Akita University, Akita, Japan.

<sup>4</sup>Research Center for Prediction of Earthquakes and Volcanic Eruptions, Tohoku University, Sendai, Japan.

<sup>5</sup>Volcanic Fluid Research Center, Tokyo Institute of Technology, Tokyo, Japan.

<sup>6</sup>Institute of Seismology and Volcanology, Hokkaido University, Sapporo, Japan.

<sup>7</sup>Disaster Prevention Research Institute, Kyoto University, Uji, Japan.

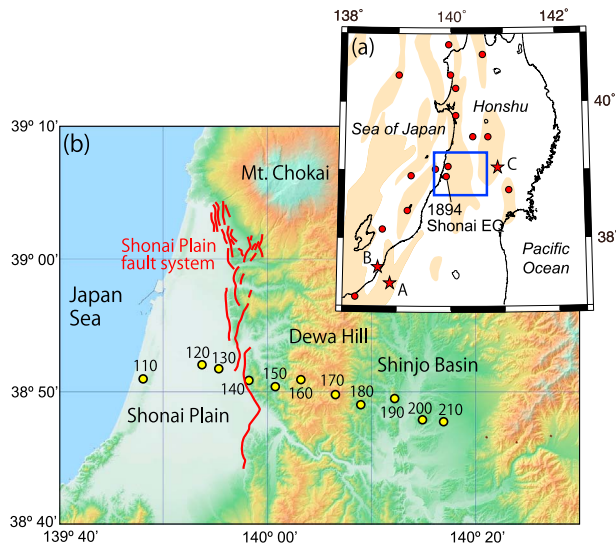


**Figure 1.** Study location. (a) Red circles denote historical intraplate earthquakes larger than  $M$  7.0 in the northeastern Honshu area [Usami, 2003]. Red stars with capital letters denote recent disastrous earthquakes: 2004 Chuetsu earthquake ( $M$  6.8) (A), 2007 Chuetsu-oki earthquake ( $M$  6.8) (B), and 2008 Iwate-Miyagi earthquake ( $M$  7.2) (C). Light orange region indicates contractional zones based on geological studies [Okamura *et al.*, 2007]. (b) Digital elevation model of the study area. MT stations in this study are shown as yellow circles with site numbers. Red lines indicate the Shonai Plain fault system [after Ikeda *et al.*, 2002].

phase tensor is defined as  $\mathbf{X}^{-1}\mathbf{Y}$ , where  $\mathbf{X}$  and  $\mathbf{Y}$  are the real and imaginary parts of the impedance tensor ( $\mathbf{Z}$ ), respectively. The orientation of the phase-tensor major axis is specified by the angle  $\alpha$ , where the phase-tensor skew angle  $\beta$  indicates the asymmetry of the phase tensor. In the ideal 2-D case,  $\beta$  equals zero, and the angle  $\alpha$  indicates the direction parallel or perpendicular to the strike of the regional 2-D structure. Thus, small  $\beta$  angles together with consistency in  $\alpha$  angles throughout the stations and frequencies can be used to judge the existence of a regional 2-D structure. Moreover, the difference between maximum and minimum phase-tensor values ( $\Phi_{\max}$  and  $\Phi_{\min}$ , respectively, defined

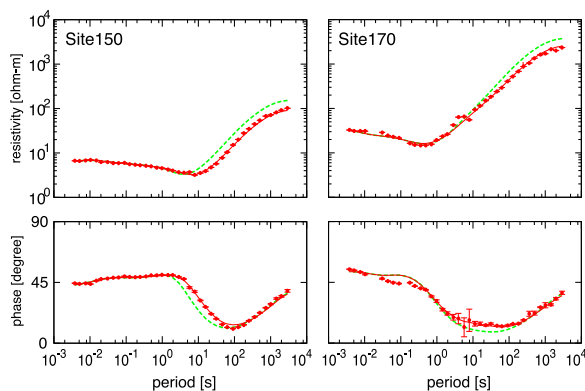


**Figure 2.** Sounding curves of apparent resistivity and phase in TM mode. Dots with error bar denote measured data. Solid and dashed lines denote the response of the inverted model and the tested model, respectively.

on the principal axes) can be used as a measure of the one-dimensional (1-D) structure.

[6] After the phase-tensor analysis, the validity of the 2-D regional structure was confirmed by the small  $\beta$  ( $1.3 \pm 5.2$  degrees) values. A significant  $\alpha$  peak appears in the rose diagram for the low-frequency band (<1 Hz) trending  $025^\circ$  (Figure 3). In contrast, the peak in the high-frequency band (>1 Hz) is roughly north trending. The high-frequency data show only a small difference between  $\Phi_{\max}$  and  $\Phi_{\min}$  (generally within  $2^\circ$ ), indicating a shallow 1-D resistivity structure. The high-frequency data are, therefore, not required to determine the 2-D strike. On the basis of the low-frequency data, there are two possibilities for the 2-D azimuth of the geo-electrical structure:  $025^\circ$  and a trend perpendicular to  $025^\circ$ . The  $025^\circ$  trend was assumed to be the strike azimuth because the induction vector in the lower frequency is dominantly oriented northwest. This orientation is parallel to the trend of geological structures and that of the nearby coastline. Previous MT surveys in northeastern Honshu, where the estimated structural trend is NNE [Ogawa *et al.*, 2001; Mishina, 2009], also support this orientation.

[7] However, thick conductive sediments with three-dimensional (3-D) configuration are distributed in the study area [Takakura, 1995]. Additionally, the combination of conductive sediment and seawater may induce strong current channeling and thereby distort the MT responses [Ichiara and Mogi, 2009]. Thus, we compared the 2-D and 3-D responses to evaluate the feasibility of 2-D approximation. A 3-D model includes the spatial distribution of real bathymetry and a replica of the conductive sediments (Figure S2). The calculated 3-D responses based on Fomenko and Mogi [2002] are markedly different from the 2-D responses in the transverse electric (TE) mode, whereas this difference is relatively small in the transverse magnetic (TM) mode (Figures S3). The difference in the TE mode is mainly due to the 3-D geometry of the conductive sediment, as described by previous studies [e.g., Wannamaker *et al.*, 1984]. Therefore, in the following 2-D inversion, we decided to use only TM-mode impedances.

[8] The estimated TM-mode apparent resistivity and phase were inverted using the 2-D inversion code developed by Ogawa and Uchida [1996]. The inversion code is based on Akaike's Bayesian information criterion least-squares method and comprehensively evaluates the root-mean-square (RMS) misfit between observed and calculated impedance, model smoothness, and static shifts. The inversion started with a 100-ohm-m homogeneous half-space model except in the seawater area where resistivity was fixed to be 0.3 ohm-m during iterations. An error floor of 5% in apparent resistivity

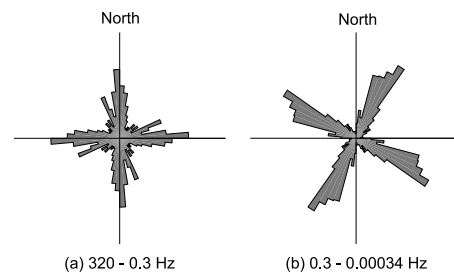


**Figure 3.** Rose diagram for  $\alpha$  azimuths derived from the phase tensor (a) between 320 and 0.3 Hz and (b) between 0.3 and 0.00034 Hz.

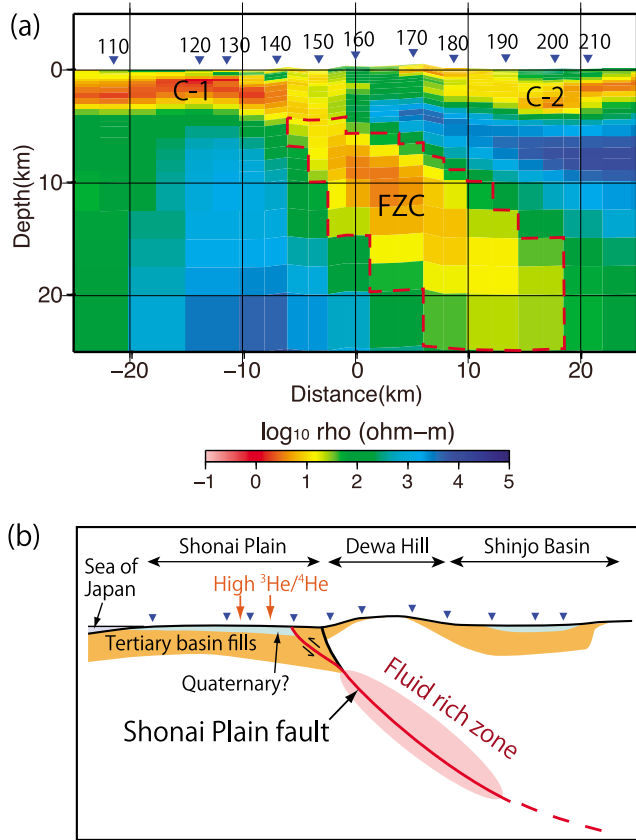


**Figure 4.** (a) Inverted resistivity profile. (b) Schematic illustration of back-arc region in central northeastern Japan.

and an equivalent error floor in phase ( $1.43^\circ$ ) were applied. The inverted model closely approximated measured impedances (Figure S1). The RMS errors were reduced to 1.66.

[9] The inverted resistivity model shows a shallow conductive layer (1–10 ohm-m) beneath the Shonai Plain and the Shinjo Basin (C-1 and C-2 in Figure 4a). This structure is present from near the surface to a depth of 4 km and is overlain by a relatively resistive layer (about 100 ohm-m); the conductive layer is absent beneath Dewa Hill. The inverted model also indicates an east-dipping, elongate conductor along the deep extension of the Shonai Plain fault zone (FZC in Figure 4a; 3–300 ohm-m). A sensitivity test supports the existence of this FZC. If the FZC (red dashed line in Figure 4a) is given a resistivity of 300 ohm-m, the calculated phases decrease by more than 5 degrees at sites 150, 160, and 170 for 0.1 Hz, as compared to measured data and the response of the inverted model (Figure 2). Because phase errors were estimated to be smaller than 1 degree at these sites and frequency, the difference is significant.

## 4. Discussion and Conclusions

### 4.1. Geological Interpretation of the Inverted Model

[10] Upper Miocene sedimentary rocks over 2000 m thick are present beneath the Shonai Plain and Shinjo Basin according to well logs and seismic surveys [Ikebe *et al.*, 1979; Sato *et al.*, 2006]. Well-logging for sedimentary units drilled 40 km north of this study's profile showed low resistivity (1–10 ohm-m [Takakura, 1995]), representing units C-1 and C-2 (Figure 4a). Lower middle Miocene mafic rocks

(Aosawa Formation) are present beneath the upper Miocene and under Dewa Hill [Sato and Amano, 1991]. Moderate resistivity (about 100 ohm-m) near the surface of Dewa Hill (sites 160–170) is consistent with resistivity logging data [Takakura, 1995].

[11] Geological studies [e.g., Sato, 1994] have suggested that back-arc opening of the Japan Sea at 13 to 25 Ma generated the Shonai Plain fault as part of a rift system in which Miocene sedimentary and volcanic rocks accumulated. When the extensional tectonic regime evolved into a compressional setting at ca. 3.5 Ma, some of the original normal faults, such as the Shonai Plain fault, were reactivated as reverse faults. This geological interpretation of the resistivity profile implies uplift of the Dewa Hill area and supports fault reactivation of the Shonai Plain fault (Figure 4). Geological studies have not imaged the deeper parts of the Shonai Plain fault, but the compressional inversion hypothesis requires an east-dipping fault beneath Dewa Hill. The east-dipping FZC is spatially consistent with the assumed fault and probably represents a fluid-filled damaged zone (discussed below). This study clarifies and supports the geological hypothesis that compressional inversion is responsible for devastating earthquakes in this area.

### 4.2. Role of Fluid in Fault Activity

[12] The temperature at the center of the FZC (3 ohm-m at 11 km depth), in the back-arc area of northeastern Japan, is estimated to be  $360^\circ\text{C}$ . Assuming a pore-fluid composition of 3.6 wt% KCl and granitic bedrock, resistivity at this temperature would be 0.04 ohm-m and  $10^6$  ohm-m, respectively [Uyeshima, 2005]. Under such conditions, the porosity at the center of the FZC (3 ohm) would be 2.0% according to the HSc model [Hashin and Shtrikman, 1962], where pore-fluid is assumed to be perfectly interconnected. The porosity would be roughly proportional to the pore-fluid resistivity because resistivity of the host rock would be much higher than that of pore fluid. The true porosity of the FZC is probably much higher than these estimates, for the following reasons. The distribution of grains and pore-fluids in the HSc model yields the most conductive condition. A lower FZC resistivity has been inferred because TM-mode data generally have low resolution and smoothness constraints are introduced in the inversion. The FZC therefore represents a fluid-filled, porous rock volume that is the product of damage along the deep extension of the Shonai Plain fault. Ogawa *et al.* [2001] also showed a conductor along the Kitayuri fault, 60 km north of the profile in the present study. The Kitayuri fault may be a continuation of the Shonai Plain fault.

[13] Numerous studies have discussed the importance of fluid in fault ruptures because pore fluids control the shear fracture strength and brittle-ductile behavior of rocks. A known mechanism for fault activity is that over-pressured fluid reduces shear strength and enhances fault slip. However, over-pressured fluid is probably not present in the Shonai Plain fault because the low-resistivity zone (FZC), which is estimated to be a high-permeability zone, is distributed continuously along the seismogenic zone and seems to be connected to the conductive sedimentary rock (C-1) for which high permeability is also assumed. The high  $^3\text{He}/^4\text{He}$  ratio (6.02 Ra) reported near the Shonai Plain fault system (Figure 4b) [Sano and Wakita, 1985; Horiguchi *et al.*, 2010] indicates the existence of a fluid path from

mantle. Because the basement of the study area mainly consists of cretaceous granite and appears to have low permeability, the FZC seems to be feasible as the fluid path.

[14] *Sibson* [2009] suggested that fault rupture due to over-pressured fluid generated high fracture permeability and fluid discharge in fault zones in northeastern Japan. The increase in the  $^3\text{He}/^4\text{He}$  ratio after the 2008 Iwate-Miyagi inland earthquake ( $M$  7.2) [*Horiguchi and Matsuda*, 2008] supports the discharge of deep fluid after the main rupture. The approximately 100-year period since the 1894 Shonai earthquake ( $M$  7.0) seems short in terms of an inland earthquake cycle. Therefore, the FZC may also experience episodic high fracture permeability and may have connected fluid-filled pore systems. The fault-valve hypothesis [*Sibson*, 1992, 2009] suggests that rupturing of a fault discharges over-pressured fluid, but over-pressured fluid develops once again with the ensuing cementation and sealing of the fault. Therefore, the FZC may eventually split into parts. Magnetotelluric surveys may detect such time-dependent changes in fault conditions because resistivity varies by some orders of magnitude depending on the connectivity of pore fluid [e.g., *Hashin and Shtrikman*, 1962]. Monitoring of these processes will help clarify the fault-rupture process.

[15] **Acknowledgments.** Landowners in the study region are thanked for permission to establish observation sites on their land. Y. Koda of the Tokyo Institute of Technology and T. Miura, R. Ikeda, K. Tsushima, N. Yagi, H. Asano, M. Omoto, and T. Kono of Akita University provided assistance with data gathering. T. Kimura of the Japan Agency for Marine-Earth Science and Technology (JAMSTEC) provided supplementary tools for inversion and sensitivity testing. Discussions with H. Sato and N. Kato of the Earthquake Research Institute, University of Tokyo, improved the paper. The manuscript was greatly improved by thoughtful comments from two anonymous reviewers. Generic Mapping Tools software [*Wessel and Smith*, 1998] was used to draw some of the figures. This research is supported by the “Multidisciplinary Research Project for High Strain Rate Zones” of the Ministry of Education, Culture, Sports, Science and Technology (MEXT), Japan.

[16] The Editor thanks two anonymous reviewers for their assistance in evaluating this paper.

## References

- Awata, T., and T. Kakimi (1985), Quaternary tectonics and damaging earthquakes in Northeast Honshu, Japan, *Earthquake Predict. Res.*, **3**, 231–251.
- Caldwell, T. G., H. M. Bibby, and C. Brown (2004), The magnetotelluric phase tensor, *Geophys. J. Int.*, **158**, 457–469, doi:10.1111/j.1365-246X.2004.02281.x.
- Fomenko, E. Y., and T. Mogi (2002), A new computation method for a staggered grid of 3D EM field conservative modeling, *Earth Planets Space*, **54**, 499–509.
- Gamble, T. D., W. M. Goubau, and J. Clarke (1979), Magnetotellurics with a remote magnetic reference, *Geophysics*, **44**, 53–68, doi:10.1190/1.1440923.
- Hashin, Z., and S. Shtrikman (1962), A variational approach to the theory of the effective magnetic permeability of multiphase materials, *J. Appl. Phys.*, **33**, 3125, doi:10.1063/1.1728579.
- Hikima, K., and K. Koketsu (2005), Rupture processes of the 2004 Chuetsu (mid-Niigata Prefecture) earthquake, Japan: A series of events in a complex fault system, *Geophys. Res. Lett.*, **32**, L18303, doi:10.1029/2005GL023588.
- Horiguchi, H., and J. Matsuda (2008), On the change of  $^3\text{He}/^4\text{He}$  ratios in hot spring gases after the Iwate-Miyagi Nairiku earthquake in 2008, *Geochemical Journal*, **42**, e1–e4.
- Horiguchi, K., S. Ueki, Y. Sano, N. Takahata, A. Hasegawa, and G. Igarashi (2010), Geographical distribution of helium isotope ratios in northeastern Japan, *Isl. Arc*, **19**, 60–70, doi:10.1111/j.1440-1738.2009.00703.x.
- Ichihara, H., and T. Mogi (2009), A realistic 3-D resistivity model explaining anomalous large magnetotelluric phases: The L-shaped conductor model, *Geophys. J. Int.*, **179**, 14–17, doi:10.1111/j.1365-246X.2009.04310.x.
- Ichihara, H., T. Mogi, H. Hase, T. Watanabe, and Y. Yamaya (2009), Resistivity and density modeling in the 1938 Kutcharo earthquake source area along a large caldera boundary, *Earth Planets Space*, **61**, 345–356.
- Ikebe, Y., A. Ozawa, and H. Inoue (1979), Geology of Sakata district, Quadrangle Series, scale 1:50,000, 77 pp., Geol. Surv. Jpn., Tsukuba.
- Ikeda, Y., T. Imaizumi, M. Togo, K. Hirakawa, T. Miyauchi, and H. Sato (Eds.) (2002), *Atlas of Quaternary Thrusts in Japan*, 254 pp., Univ. of Tokyo Press, Tokyo.
- Mishina, M. (2009), Distribution of crustal fluids in northeast Japan as inferred from resistivity surveys, *Gondwana Res.*, **16**, 563–571, doi:10.1016/j.gr.2009.02.005.
- Ogawa, Y., and T. Uchida (1996), A two-dimensional magnetotelluric inversion assuming Gaussian static shift, *Geophys. J. Int.*, **126**, 69–76, doi:10.1111/j.1365-246X.1996.tb05267.x.
- Ogawa, Y., et al. (2001), Magnetotelluric imaging of fluids in intraplate earthquake zones, NE Japan back arc, *Geophys. Res. Lett.*, **28**, 3741–3744, doi:10.1029/2001GL013269.
- Okamura, Y., T. Ishiyama, and Y. Yanagisawa (2007), Fault-related folds above the source fault of the 2004 mid-Niigata Prefecture earthquake, in a fold-and-thrust belt caused by basin inversion along the eastern margin of the Japan Sea, *J. Geophys. Res.*, **112**, B03S08, doi:10.1029/2006JB004320.
- Sano, Y., and H. Wakita (1985), Geographical distribution of  $^3\text{He}/^4\text{He}$  ratios in Japan: Implications for arc tectonics and incipient magmatism, *J. Geophys. Res.*, **90**, 8729–8741, doi:10.1029/JB090iB10p08729.
- Sato, H. (1994), The relationship between late Cenozoic tectonic events and stress field and basin development in northeast Japan, *J. Geophys. Res.*, **99**, 22,261–22,274, doi:10.1029/94JB00854.
- Sato, H., and K. Amano (1991), Relationship between tectonics, volcanism, sedimentation and basin development, late Cenozoic, central part of northern Honshu, Japan, *Sediment. Geol.*, **74**, 323–343, doi:10.1016/0037-0738(91)90071-K.
- Sato, H., et al. (2006), Seismic reflection profiling across active folds in the eastern Shinjo basin, NE Japan, *Bull. Earthquake Res. Inst. Univ. Tokyo*, **81**, 157–169.
- Sibson, R. H. (1992), Implications of fault-valve behaviour for rupture nucleation and recurrence, *Tectonophysics*, **211**, 283–293, doi:10.1016/0040-1951(92)90065-E.
- Sibson, R. H. (2007), An episode of fault-valve behaviour during compressional inversion?—The 2004 MJ6.8 Mid-Niigata Prefecture, Japan, earthquake sequence, *Earth Planet. Sci. Lett.*, **257**, 188–199, doi:10.1016/j.epsl.2007.02.031.
- Sibson, R. H. (2009), Rupturing in overpressured crust during compressional inversion—The case from NE Honshu, Japan, *Tectonophysics*, **473**, 404–416, doi:10.1016/j.tecto.2009.03.016.
- Takakura, S. (1995), Resistivity of Neogene rocks on the Niigata and the Akita oil fields, Japan, *Butsuri Tansa*, **48**, 161–175.
- Usami, T. (2003), *Materials for Comprehensive List of Destructive Earthquakes in Japan*, Univ. of Tokyo Press, Tokyo.
- Uyeshima, M. (2005), Estimation of water volume fraction in the crust from electrical conductivity structure, *J. Geogr.*, **114**, 862–870.
- Uyeshima, M., et al. (2005), Resistivity imaging across the source region of the 2004 mid-Niigata Prefecture earthquake ( $M$ 6.8), central Japan, *Earth Planets Space*, **57**, 441–446.
- Wannamaker, P. E., G. W. Hohmann, and S. H. Ward (1984), Magnetotelluric responses of three-dimensional bodies in layered earths, *Geophysics*, **49**, 1517–1533, doi:10.1190/1.1441777.
- Wannamaker, P. E., T. G. Caldwell, G. R. Jiracek, V. Maris, G. J. Hill, Y. Ogawa, H. M. Bibby, S. L. Bennie, and W. Heise (2009), Fluid and deformation regime of an advancing subduction system at Marlborough, New Zealand, *Nature*, **460**, doi:10.1038/nature08204.
- Wessel, P., and W. H. F. Smith (1998), New, improved version of the Generic Mapping Tools released, *Eos Trans. AGU*, **79**, 579, doi:10.1029/98EO00426.
- Yoshimura, R., et al. (2008), Magnetotelluric observations around the focal region of the 2007 Noto Hanto earthquake ( $M$ 6.9), central Japan, *Earth Planets Space*, **60**, 117–122.
- H. Ichihara, Japan Agency for Earth-Marine Science and Technology, 2-15 Natsushima, Yokosuka, Kanagawa 237-0061, Japan. (h-ichi@jamstec.go.jp)
- M. Mishina, Research Center for Prediction of Earthquakes and Volcanic Eruptions, Tohoku University, 6-6 Aramaki, Aoba-ku, Sendai, Miyagi 980-8578, Japan.
- Y. Morita, T. Ogawa, Y. Usui, M. Uyeshima, A. Watanabe, and Y. Yamaya, Earthquake Research Institute, University of Tokyo, 1-1-1, Yayoi, Bunkyo-ku, Tokyo 113-0032, Japan.
- T. Nishitani and S. Sakanaka, Faculty of Engineering and Resource Science, Akita University, 1-1 Gakuen-machi, Tegata, Akita 010-8502, Japan.
- Y. Ogawa, Volcanic Fluid Research Center, Tokyo Institute of Technology, 2-12-1 Ookayama, Meguro, Tokyo 152-8551, Japan.
- R. Yoshimura, Disaster Prevention Research Institute, Kyoto University, Gokasho, Uji, Kyoto 611-0011, Japan.